NANO LETTERS

2003
Vol. 3, No. 6
757−760

Nanopatterning of "Hard" Magnetic Nanostructures via Dip-Pen Nanolithography and a Sol-Based Ink

Lei Fu,[†,§] Xiaogang Liu,[‡,§] Yi Zhang,[‡] Vinayak P. Dravid,*[,†] and Chad A. Mirkin*[,‡]

Department of Materials Science and Engineering and Institute for Nanotechnology, Northwestern University, 2220 Campus Drive, Evanston, Illinois 60208-3113, and Department of Chemistry and Institute for Nanotechnology, Northwestern University, 2145 Sheridan Road, Evanston, Illinois 60208-3113

Received March 20, 2003; Revised Manuscript Received April 8, 2003

ABSTRACT

A direct-write method for fabricating "hard" magnetic barium hexaferrite, $BaFe_{12}O_{19}$ (BaFe), nanostructures, based on dip-pen nanolithography and a sol−gel process, is presented. This method utilizes a conventional atomic force microscope tip, coated with the BaFe precursor solution, to generate patterns that can be post-treated at elevated temperature to generate magnetic features consisting of barium ferrite in its hexagonal magnetoplumbite (M-type) structure. Features ranging from several hundred nm down to below 100 nm were generated and studied using AFM, magnetic force microscopy, and X-ray photoelectron spectroscopy. The approach offers a new way for patterning functional inorganic nanostructures with deliberate control over feature size and shape, as well as interfeature distance and location.

Over the past decade, there has been considerable interest in methods for synthesizing and patterning nanoscale magnetic materials. In addition to exhibiting novel size-dependent properties,[1−5] these materials (particularly ones with high coercivities and mechanical stabilities, i.e., "hard" magnets) are being explored as potential media for high-density recording.[6−8] Two of the main challenges in this field are: (a) site- and shape-specific patterning of hard magnetic nanostructure on the sub-100 nm scale, and (b) ability to reliably and reproducibly read/write such minute features.[7] The conventional top-down approach in recording media is plagued by the difficulties of etching and patterning novel hard magnetic systems, especially as the individual recording elements approach the superparamagnetic limit at room temperature operations. The ability to read/write such nanostructures is equally challenging, but progress is also being made on this front with new approaches and instrumentation such as quasistatic write/read testing of perpendicular patterned media and analogous versions of the IBM millipede reader.[9] As the demand for increased areal density for recording media increases, isolating patterned recording segments may prove to be a useful approach to not only enhance aerial densities of magnetic bits but also to ensure minimal "cross-talk" via physical separation of bit segments. Perhaps more importantly, magnetic nanostructures are finding novel applications in the fields of biotechnology and integrated magnetoelectronics,[5] where the ability to pattern magnetic nanostructures is essential.

Barium hexaferrite (BaFe), in particular, is a good hard magnet candidate for high-density media, and it also serves as a "model" hard magnet with complex structure. It is challenging to achieve high-resolution patterning of BaFe by conventional lithography and etching processes.[10,11] Focused ion beam (FIB) patterning is a viable proof-of-concept approach, as was recently demonstrated by Albretch,[9] but methods that allow one to pattern such structures *directly* with deliberate control over feature location, size, and shape are desirable. Herein we report a novel direct-write nanopatterning method for BaFe, based upon dip-pen nanolithography (DPN)[12−19] and a sol−gel process.[20,21]

DPN experiments were carried out under ambient conditions (31% relative humidity and 24 °C) with a Thermomicroscopes CP AFM and commercial cantilevers (force constant = 0.05 N/m, Si_3N_4). To minimize piezo tube drift problems, a 90-μm scanner with closed loop scan control was used for all of the DPN experiments. AFM and MFM measurements were made in air using a Digital Instruments Multimode Nanoscope IIIa with an extender electronics module in tapping and lift modes, respectively.

We generated BaFe nanostructures on a silicon oxide substrate according to the following procedure (Figure 1).

* Corresponding author. E-mail: v-dravid@northwestern.edu; camirkin@chem.northwestern.edu

† Department of Materials Science and Engineering and Institute for Nanotechnology.

‡ Department of Chemistry and Institute for Nanotechnology.

§ These authors contributed equally to this work.

10.1021/nl034172g CCC: $25.00
Published on Web 04/30/2003

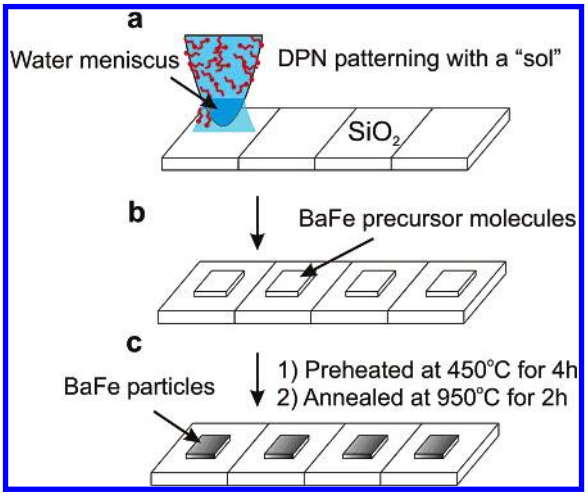

Figure 1. Schematic diagram depicting the patterning of magnetic BaFe nanostructures on silicon oxide. (a) An atomic force microscope (AFM) tip coated with a precursor solution of barium ferrite is brought into contact with the silicon oxide substrate. (b) The solution is transferred to the substrate as the tip is traversed across it. (c) Post-annealing yields the desired BaFe nanostructures.

The surface of a SiO_2/Si wafer is first patterned via DPN (contact force 2.5 nN) using a conventional atomic force microscope (AFM) cantilever coated with a BaFe precursor solution that contains a mixture of iron nitrate ($Fe(NO_3)_3 \cdot 9H_2O$; 0.0115 mol) and barium carbonate ($BaCO_3$; 0.001 mol) in ethylene glycol ($HOCH_2CH_2OH$; 25 mL). Unless otherwise noted, all chemicals and solvents were purchased from Sigma-Aldrich. The ethylene glycol not only dissolves and stabilizes the starting materials but also wets the hydroxylated substrate, a factor that is important in the nanopatterning process. Indeed, we did not get comparable results with 2-propanol, water, methanol, or ethanol as the solvents under nearly identical conditions. The patterns are preheated at 450 °C for 4 h and then annealed at 950 °C in an air atmosphere for 2 h, ultimately yielding BaFe nanostructures. Based on literature precedent,[10] the key reactions involving the BaFe transformation are assumed to be the following:

$$2Fe(NO_3)_3 \rightarrow Fe_2O_3 + 3N_2O_5\uparrow$$

$$BaCO_3 + Fe_2O_3 \rightarrow BaFe_2O_4 + CO_2\uparrow$$

$$BaFe_2O_4 + 5Fe_2O_3 \rightarrow BaFe_{12}O_{19}$$

To compare the chemical and structural properties of the nanostructures with BaFe, bulk samples of BaFe particles and films were prepared by the aforementioned sol−gel method. The X-ray diffraction (XRD) pattern of the as-synthesized BaFe particles shows a series of Bragg reflections that can be well indexed as M-type hexagonal BaFe (Figure 2a). In contrast, the XRD pattern of the sample without preheating shows peaks corresponding to the α-Fe_2O_3 phase (Figure 2b). The size, morphology, and crystal structure of the BaFe particles were also investigated with a HF-2000 field emission gun (FEG) transmission electron microscope

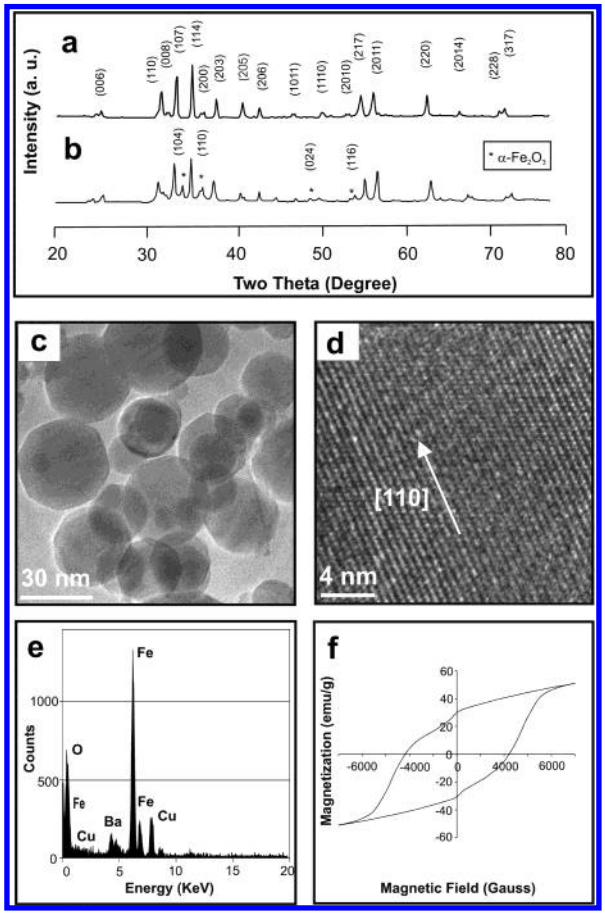

Figure 2. Characterization of the bulk BaFe particle samples. (a) XRD pattern of as-synthesized BaFe particles. The indexing is based on tabulated hexagonal $BaFe_{12}O_{19}$ reflections. (b) XRD spectrum of BaFe particles synthesized without the preheating step. (c) Transmission electron microscope (TEM) image of as-synthesized BaFe particles. (d) High-resolution TEM image showing single-crystal nature of these particles. (e) Energy-dispersive X-ray spectroscopy (EDXS) spectrum obtained from these nanoparticles. The signal for Cu comes from the copper grid on which these particles were supported. (f) Magnetic hysteresis loop measurements of the BaFe nanoparticles at room temperature.

(TEM). The polygonal particles have a mean diameter of ~35 nm (Figure 2c). High resolution TEM shows the lattice image of a BaFe particle viewed along the [110] projection, Figure 2d. Elemental analysis, using energy-dispersive X-ray spectroscopy (EDS) operating in the STEM mode, confirmed the presence of Ba, Fe, and O in individual nanoparticles as well as aggregate structures (Figure 2e). The magnetic properties of the BaFe nanoparticles were investigated at room temperature by superconducting quantum interference device magnetometry (SQUID, Quantum Design, MPMS). The magnetic nanoparticles exhibit a hysteresis loop (though not fully saturated), a reasonably high coercivity (4250 G), and a large remanent magnetization (32.2 emu/g), which is reasonably consistent with earlier reports on BaFe particles (Figure 2f).[10,11]

In a typical DPN nanopatterning experiment, the BaFe precursor solution in ethylene glycol was prepared and sonicated for 15 min before being used. Silicon oxide wafers were cleaved into to 0.5 in. × 0.5 in. squares and sonicated

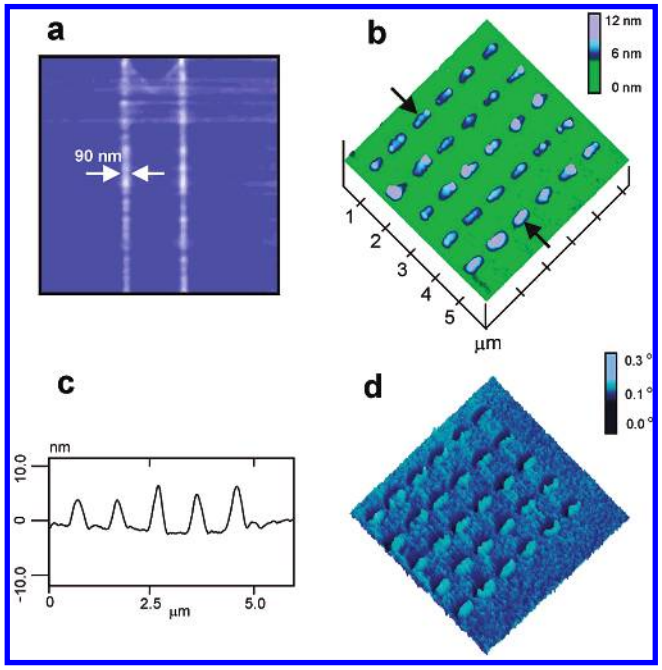

Figure 3. Scanning probe microscope (SPM) studies of the BaFe patterns. (a) Topographic AFM image of magnetic BaFe lines on the silicon oxide substrate. The speed for the BaFe precursor deposition is 0.2 μm/s. (b) Topographic AFM image of an array of magnetic bars. The deposition speed is 0.1 μm/s. (c) Cross-sectional topography trace of a line (marked by the arrows in b). (d) Magnetic force microscope (MFM) image obtained from these magnetic bars.

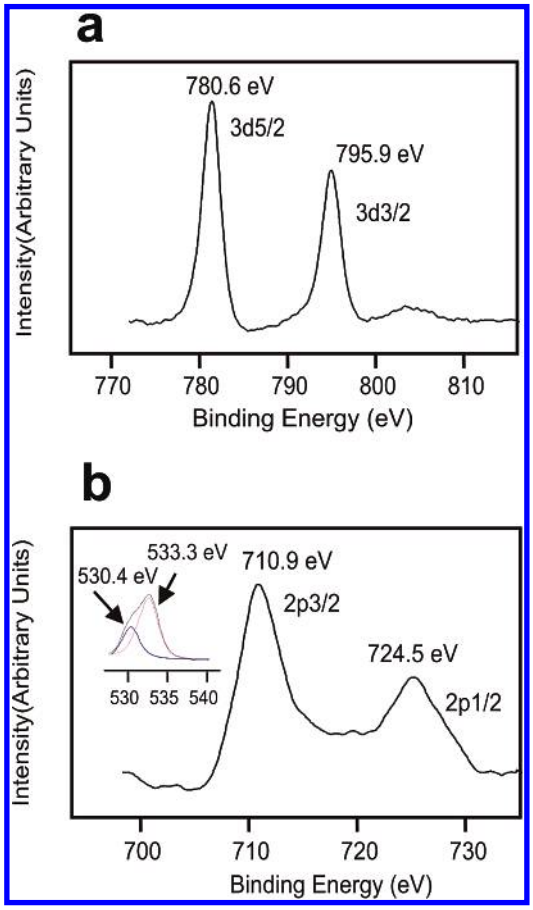

Figure 4. X-ray photoelectron spectroscopy (XPS) characterization of the patterned substrate. (a) Barium peaks were detected from the silicon oxide substrate using XPS. (b) Iron peaks detected from the same sample (inset: oxygen peaks and the deconvolution result).

in dichloromethane, methanol, and Nanopure water for 10 min, respectively. The wafers were then immersed in freshly mixed ammonium hydroxide/peroxide solution (NH_4OH/H_2O_2/H_2O, v:v:v = 1:1:5) for 1 h at about 100 °C, after which time they were rinsed in Nanopure water. The wafers were dried in N_2 gas before immersion in the different solvents. A conventional silicon nitride AFM microcantilever was then dipped into the solution for 1 min. The cantilever was blown dry with compressed difluoroethane to remove residual solvent from the ink on the AFM tip. The barium ferrite precursor solution was deposited on a SiO_2/Si substrate by bringing the coated AFM tip in contact with the surface and then moving it across the substrate, using nanolithography software (DPN−Write, NanoInk, Inc., Chicago, IL). The aforementioned post-treatment procedure was used to generate all patterns reported herein (Figure 3). With this strategy, magnetic nanostructures with dimensions ranging from several hundred nanometers down to 90 nm could be routinely generated.

When a magnetic material is patterned into arrays in the form of nanosized dots, bars, or columns on a nonmagnetic matrix, each feature may contain one or, at most, a few domains in contrast to the multigrain structure of present conventional storage medium (for example, in magnetic thin film media, each bit consists of usually several grains, all typically represent single domain).[8] The patterned media in such isolated-patterned structures remain stable down to much lower lateral dimensions than conventional bits in continuous media.[8,9] Lines of BaFe with an average width of 90 nm were generated via the combined DPN-sol gel approach (Figure 3a). Arrays of magnetic BaFe bars that have an average area of 215 × 465 nm^2 with an average height of 6.7 nm were also generated by controlling the tip−substrate scan speed (Figure 3b,c). The magnetic properties of the nanopatterns were further examined by magnetic force microscopy (MFM) in lift mode. Before imaging, the tip, coated with a ferromagnetic thin film of cobalt, was magnetized with an external magnetic field. The magnetic force was then detected by measuring the phase shift in the cantilever oscillation, a consequence of the magnetic interactions acting on the tip. The MFM image indicates that these patterns are indeed magnetic (Figure 3d), reflected in the deflection of the tip during MFM imaging. Note that such experiments merely indicate the presence of magnetically active nanostructures, and detailed information about quantitative magnetization, and the roles of crystallographic and magnetic anisotropy are not obtained from such experiments. The experiment confirms the presence of local magnetism in such "nanodisk" features and is consistent with the structural and chemical analysis of BaFe below.

The elemental composition of the BaFe formed via DPN was determined by investigating large area features (500 × 500 μm^2) by X-ray photoelectron spectroscopy (XPS). XPS spectra were recorded using an Omicron ESCA probe operated in vacuum at around 4.8 × 10^{-10} Torr with monochromated Al Kα radiation (1486.6 eV, 300 W). Binding energies were corrected by referencing the C1s

signal of adventitious hydrocarbon to 284.8 eV. The electron-pass energy in the analyzer was set at 50 eV. The $Ba3d_{5/2}$ and $Ba3d_{3/2}$ peaks were observed at 780.6 and 795.9 eV respectively, which were the characteristic values for $BaFe_{12}O_{19}$ (Figure 4a). The $Fe2p_{3/2}$ and $Fe2p_{1/2}$ peaks were observed at 710.9 and 724.5 eV respectively, which were diagnostic of BaFe (Figure 4b). The O1s spectrum showed a large fwhm of 2.5 eV, which was broadened on the low binding-energy side (Figure 4b (inset)). The O1s spectrum could be resolved into two peaks using a least-squares curve fitting method with a mixture of Gaussian and Lorentzian functions on a Shirley-type background.[22] The low binding-energy peak at 530.4 eV represents the O^{2-} contribution in the $BaFe_{12}O_{19}$, while the peak at high binding energy of 533.3 eV is attributed to the OH^- on hydroxylated surface of silicon dioxide.[23]

In summary, proof-of-concept experiments have shown that it is possible to construct barium ferrite nanostructures, based on a combination of a novel sol−gel process and the DPN method. The combined approach, which takes into account the versatility and attributes of DPN (direct-writing, feature shape and size control, and soft matter compatibility), should pave the way for constructing sophisticated architectures of magnetic nanostructures that can provide further insight into the field of magnetoelectronic sensor devices and may even lead to high-density information storage systems with proper control over size, shape, and anisotropy of individual features. Indeed, modest estimates, based on the feature size attainable via such an approach, suggest a potential density of greater than 150 Gb/in^2. The realization of such an advance will also depend on the parallelization of DPN, which is well on its way.[24]

Acknowledgment. The authors acknowledge the AFOSR-MURI, DARPA, and NSF-NSEC for support of this research.

References

(1) Sorensen, C. M. *Nanoscale Materials in Chemistry*; Wiley: New York, 2001.
(2) Sun, S.; Murray, C. B.; Weller, D.; Folks, L.; Moser, A. *Science* **2000**, *287*, 1989.
(3) Edelstein, R. L.; Tamanaha, C. R.; Sheehan, P. E.; Miller, M. M.; Baselt, D. R.; Whitman, L. J.; Colton, R. J. *Biosens. Bioelectron.* **2000**, *14*, 805.
(4) Xia, Y.; Rogers, J. A.; Paul, K.; Whitesides, G. M. *Chem. Rev.* **1999**, *99*, 1823.
(5) Freeman, M. R.; Choi, B. C. *Science* **2001**, *16*, 1484.
(6) New, R. M. H.; Pease, R. F. W.; White, R. L. *J. Vac. Sci. Technol. B* **1994**, *12*, 3196.
(7) Chou, S. Y.; Krausss, P. R.; Kong, L. *J. Appl. Phys.* **1996**, *79*, 6101.
(8) O'Grady, K.; Laidler, H. *J. Magn. Magn. Mater.* **1999**, *200*, 616.
(9) Albrecht, M.; Rettner, C. T.; Moser, A.; Best, M. E.; Terris, B. D. *Appl. Phys. Lett.* **2002**, *81*, 2875.
(10) Hylton, T. L.; Parker, M. A.; Howard, J. K. *Appl. Phys. Lett.* **1992**, *61*, 867.
(11) Ishikawa, A.; Tanahashi, K.; Futamoto, M. *J. Appl. Phys.* **1996**, *79*, 7080.
(12) Piner, R. D.; Zhu, J.; Xu, F.; Hong, S.; Mirkin, C. A. *Science* **1999**, *283*, 661.
(13) Maynor, B. W.; Li, Y.; Liu, J. *Langmuir* **2001**, *17*, 2575.
(14) Li, Y.; Maynor, B. W.; Liu, J. *J. Am. Chem. Soc.* **2001**, *123*, 2105.
(15) Noy, A.; Miller, A. E.; Klare, J. E.; Weeks, B. L.; Woods, B. W.; DeYoreo, J. J. *Nano Lett.* **2002**, *2*, 109.
(16) Liu, X.; Fu, L.; Hong, S.; Dravid, V. P.; Mirkin, C. A. *Adv. Mater.* **2002**, *14*, 231.
(17) McKendry, R.; Huck, W. T. S.; Weeks, B.; Fiorini, M.; Abell, C.; Rayment, T. *Nano Lett.* **2002**, *2*, 713.
(18) Porter, L. A., Jr.; Choi, H. C.; Schmeltzer, J. M.; Ribbe, A. E.; Elliott, L. C. C.; Buriak, J. M. *Nano Lett.* **2002**, *2*, 1369.
(19) Agarwal, G.; Sowards, L. A.; Naik, R. R.; Stone, M. O. *J. Am. Chem. Soc.* **2003**, *125*, 580.
(20) Yang, P.; Deng, T.; Zhao, D.; Feng, P.; Pine, D.; Chmelka, B.; Whitesides, G.; Stucky, G. *Science* **1998**, *282*, 2244.
(21) Zhong, W.; Ding, W.; Zhang, N.; Hong, J.; Yan, Q.; Du, Y. *J. Magn. Magn. Mater.* **1997**, *168*, 196.
(22) Briggs, D.; Seah, M. P. *Practical Surface Analysis*; Wiley: Chichester, 1990.
(23) Duval, Y.; Mielczarski, J. A.; Pokrovsky, O. S.; Mielczarski, E.; Ehrhardt, J. J. *J. Phys. Chem. B* **2002**, *106*, 2937.
(24) Zhang, M.; Bullen, D.; Chung, S.-W.; Hong, S.; Ryu, K. S.; Fan, Z.; Mirkin, C. A.; Liu, C. *Nanotech.* **2002**, *13*, 212.

NL034172G